

# A criterion to detect line plumes from velocity fields in turbulent convection

Koothur Vipin<sup>†</sup> and Baburaj A. Puthenveettil

Department of Applied Mechanics, Indian Institute of Technology Madras, Chennai 600036, India

(Received ?; revised ?; accepted ?. - To be entered by editorial office)

We present a simple, new criterion to extract line plumes from the velocity fields, without using the temperature field, in a horizontal plane close to the plate in turbulent convection. The existing coherent structure detection criteria from velocity fields, proposed for shear driven wall turbulence, are first shown to be inadequate for turbulent convection. Based on physical arguments, we then propose that the negative values of  $\overline{\nabla_H \cdot \bar{u}}$ , the horizontal divergence of the horizontal velocity field extracts the plume regions from the velocity field. The  $\overline{\nabla_H \cdot \bar{u}}$  criterion is then shown to predict the total length of plumes correctly over a Rayleigh number range of  $7.7 \times 10^5 \leq Ra_w \leq 1.43 \times 10^9$  and a Prandtl number range of  $3.96 \leq Pr \leq 5.3$ . The thickness of the plume region predicted by the present criterion is approximately same as that obtained by a threshold of RMS temperature fluctuations,  $\sqrt{T'^2} = 0.2\Delta T$ , where  $\Delta T$  is the temperature drop across the fluid layer.

**Key words:**

---

## 1. Introduction

Persistent line plumes are the dominant coherent structures on hot surfaces in turbulent convection (Theerthan & Arakeri 1994). The spatial distribution of such line plumes on the hot plate have been studied mostly by observing concentration of dyes (Sparrow & Husar 1969; Adrian, Ferreira & Boberg 1986; Theerthan & Arakeri 1998; Puthenveettil 2004; Puthenveettil, Ananthakrishna & Arakeri 2005; Puthenveettil, Gunasegarane, Agrawal, Schmeling, 2011; Gunasegarane & Puthenveettil 2014) or by visualizing temperature sensitive tracers like liquid crystals (Zhou & Xia 2002). The plume structure has also been obtained by Shiskina & Wagner (2008) using criteria like conditional averaged values on temperature of vertical velocity, absolute value of horizontal velocity, heat flux, thermal dissipation rates and the vertical and horizontal vorticity components. As per them, a threshold of conditional averaged thermal dissipation rates on temperature are the best for extracting plumes from numerical simulations. At a location, plumes have been detected temporally by analysing the temperature signals (Belmonte & Libchaber 1996) as well as the conditional averaged velocity on the temperature (Ching, Guo, Shang, Tong & Xia 2004). To apply all the above methods and obtain the spatial pattern of line plumes, one needs scalar fields like temperature or concentration, often along with the 3D velocity fields. In experimental studies, only the velocity fields are available, as in most particle imaging velocimetry (PIV) studies; these methods are hence unsuitable to detect the spatial pattern of line plumes.

<sup>†</sup> Email address for correspondence: vipink159@gmail.com

Detection of coherent structures using velocity fields alone have been extensively studied in wall flows where turbulence is solely produced by shear (Tardu (2014)). Some of the criteria used in these flows include  $Q$ -criterion (Hunt, Wray & Moin 1988),  $\lambda_2$  criterion (Jeong & Hussain 1995) and swirling strength ( $\lambda_{ci}$ ) method (Zhou, Adrian, Balachandar & Kendall 1999). All these methods are based on the local analysis of the velocity gradient tensor  $\overline{\nabla \mathbf{u}}$ , often using all its nine components. To get all the components of  $\overline{\nabla \mathbf{u}}$ , one needs the three velocity components and the three gradients of each of the velocity components, all of these are most often not available in experimental studies. For most stereo PIV studies, the three velocity components and their horizontal gradients in a plane are only available; the data is further limited to the two horizontal components of velocities and their horizontal gradients for 2D PIV. In such cases, to detect coherent structures in wall shear turbulence, the above criteria are calculated with the unavailable components of  $\overline{\nabla \mathbf{u}}$ , often the components that use the vertical gradients of velocity, set to zero; the approximation seems to work fairly well for wall shear flows. Such an approximation however appears unrealistic near the hot, horizontal plate in convection where vertical gradients are predominant when vertical rising structures like plumes are present.

In this study we propose and demonstrate a simple, new criterion which is able to extract line plumes using just the horizontal velocity field in a plane parallel and close to the hot plate in turbulent convection for a Rayleigh number range of  $7.7 \times 10^5 \leq Ra_w \leq 1.43 \times 10^9$  and a Prandtl number range of  $3.96 < Pr < 5.3$  where,  $Ra_w = g\beta\Delta T_w H^3/\nu\alpha$  and  $Pr = \nu/\alpha$  with  $\Delta T_w$  being the temperature drop near the plate;  $\Delta T_w$  is half  $\Delta T$ , the temperature drop across the fluid layer height  $H$ ,  $\nu$  and  $\alpha$  the coefficients of kinematic viscosity and molecular diffusivity,  $g$  the acceleration due to gravity and  $\beta$  the coefficient of thermal expansion. The proposed criterion of negative values of horizontal divergence of the horizontal velocity field has the advantages that it is simple to compute from velocity fields in a plane parallel and close to the plate, it does not need the vertical gradients of velocities, it needs only the spatial distribution of horizontal velocity components, it does not need temperature fields and that it does not need any arbitrary threshold value that varies from flow to flow. Such a criterion will be very useful in detecting line plumes in PIV studies of the velocity field near the plate in turbulent convection. The paper is organised as follows, we first describe the setup and PIV diagnostics used to obtain the velocity field in a horizontal plane close to the hot plate in §2. The criteria used in wall shear turbulence is then applied to this velocity field to show their inadequacy in §3.1. The new criterion is then proposed based on physical considerations in §3.2.1 and then verified in §3.2.2.

## 2. Experiment

### 2.1. Apparatus

The velocity field measurements were conducted for unsteady temperature driven convection in water in an open top glass tank of cross sectional area  $300 \times 300 \text{ mm}^2$  and height of 250 mm insulated on the sides as shown in Figure 1a. The constant heat flux through the bottom, horizontal, copper plate and the water layer height  $H$  were changed to achieve the range of  $Ra_w$  and  $Pr$  shown in table 1. The heat flux was provided by a nichrome wire heater sandwiched between two aluminum plates and connected to a variac. The temperature difference ( $T_1 - T_2$ ) across a glass plate, placed between the upper aluminum plate and the copper plate was measured using T-type thermocouples to estimate the heat flux. The temperature difference between the bottom plate and the bulk  $T_w - T_B = \Delta T_w$  was measured using thermocouples kept touching the copper plate

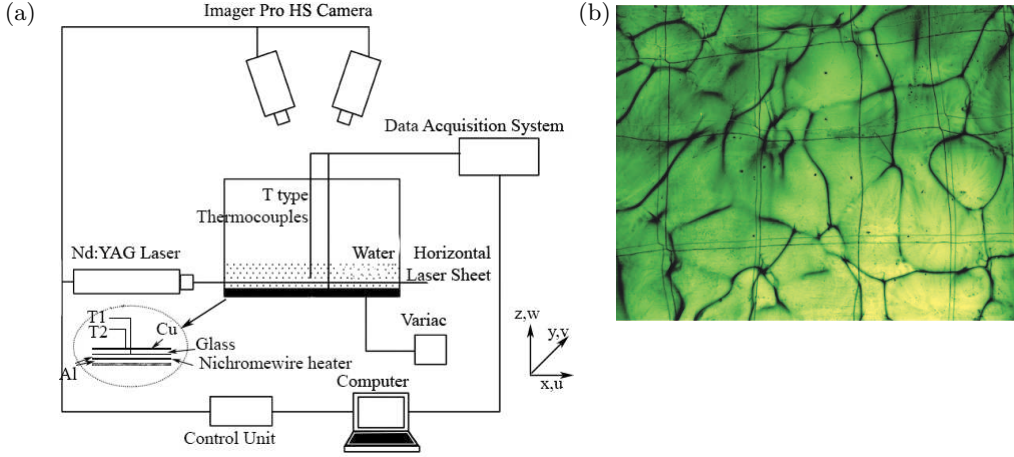


Figure 1: (a), Schematic of the present experimental setup; (b), Line plumes at  $Ra_w = 7.5 \times 10^5$  detected by electrochemical dye visualization (Puthenveettil, Gunasegarane, Agrawal, Schmeling, Bosbach & Arakeri 2011).

| $Ra_w$<br>$\times 10^7$ | $Pr$ | $\Delta T_w$<br>$^\circ C$ | $T$<br>$^\circ C$ | $\nu$<br>$\times 10^{-7}$<br>$m^2 s^{-1}$ | $\alpha$<br>$\times 10^{-7}$<br>$m^2 s^{-1}$ | $H$<br>mm | $\delta_{pb}$<br>mm | $\delta_{nc}$<br>mm | $h_m$<br>mm | $A_i$<br>$mm^2$  | $t_p$<br>mm | $\Delta t$<br>s | $D_I$<br>pix | over-<br>lap<br>% | $L_v$<br>mm |
|-------------------------|------|----------------------------|-------------------|---|--|-----------|---------------------|---------------------|-------------|------------------|-------------|-----------------|--------------|-------------------|-------------|
| 0.0766                  | 5.3  | 0.26                       | 30                | 7.99                                      | 1.502  | 50        | 33.68               | 4.8                 | 3.5         | $80 \times 80$   | 9.05        | 0.2             | 32           | 0                 | 1.27        |
| 0.384                   | 5.19 | 1.26                       | 31                | 7.82                                      | 1.508  | 50        | 23.29               | 2.75                | 2           | $145 \times 110$ | 7.93        | 0.2             | 32           | 50                | 2.12        |
| 3.40                    | 4.96 | 1.30                       | 33                | 7.51                                      | 1.51   | 100       | 14.08               | 2.6                 | 2           | $85 \times 65$   | 7.75        | 0.1             | 32           | 50                | 1.08        |
| 7.29                    | 4.75 | 2.6                        | 35                | 7.22                                      | 1.518  | 100       | 11.70               | 1.97                | 1.5         | $85 \times 65$   | 7.05        | 0.1             | 32           | 50                | 1.08        |
| 13.2                    | 4.28 | 4                          | 40                | 6.57                                      | 1.53   | 100       | 9.88                | 1.53                | 1.2         | $85 \times 65$   | 6.24        | 0.1             | 32           | 50                | 1.08        |
| 58.1                    | 4.86 | 2.68                       | 34                | 7.36                                      | 1.51   | 200       | 7.41                | 1.99                | 1.4         | $145 \times 110$ | 7.06        | 0.0667          | 64           | 75                | 1.8         |
| 143                     | 3.96 | 4.8                        | 44                | 6.11                                      | 1.54   | 200       | 5.64                | 1.32                | 1.2         | $145 \times 110$ | 6.03        | 0.0625          | 64           | 75                | 1.8         |

Table 1: Values of experimental parameters, length scales and PIV parameters.  $T$  is the temperature of the bulk fluid,  $D_I$  is one side of the square interrogation window.

and in the bulk fluid. Measurements were made only after a quasi-steady state was attained after around 3 hrs, in which  $\Delta T_w$  remained a constant, as monitored by a data logger (Agilent, model 34970A). For more details of the setup, the reader is referred to Gunasegarane & Puthenveettil (2014).

## 2.2. Diagnostics

The velocity field in a horizontal (x-y) plane, parallel and close to the hot copper plate at the bottom was obtained by stereo PIV at all  $Ra_w$ , except at  $Ra_w = 7.66 \times 10^5$ , where 2D PIV was used. The copper plate was painted black to prevent reflection of light from its surface. As could be seen from table 1, the height of the measurement plane above the hot plate ( $h_m$ ) was chosen to be within the Prandtl-Blasius velocity boundary layer thickness ( $\delta_{pb}$ ) and within the natural convection velocity boundary layer thickness ( $\delta_{nc}$ ), estimated from Ahlers *et al.* (2009) and Puthenveettil *et al.* (2011). The flow was seeded with poly-amide spheres (mean diameter  $d_p = 55 \mu m$  and density  $\rho_p = 1.012 g cm^{-3}$ ), which were illuminated by a laser sheet of thickness 1 mm from a Nd:YAG laser (Litron, 100 mJ/pulse). The value of the particle Stokes number, the ratio of particle relaxation

time and the characteristic time scale of the flow, was less than 0.0024; the particles hence followed the flow. Two Imager Pro HS (LaVision GmbH) cameras with  $1024 \times 1280$  pixel resolution (Imager Pro with resolution of  $2048 \times 2048$  pixels for the 2D2C experiment) were used to capture the particle images of area  $A_i$  at the center of the plate so that  $A_i$  had at least 8 to 12 plumes; the values of  $A_i$  are shown in table 1. The cameras with the Scheimpflug adapters were kept at an inclination of  $25^\circ$  with the  $z$  axis, with the depth of field at around 2 mm, greater than the laser sheet thickness. A single pulse, single frame mode was used to capture the particle images with the laser pulse separation  $\Delta t$  chosen such that the highest out of plane particle displacement, due to the center line plume velocity, was not more than one fourth of the laser sheet thickness. The maximum in-plane particle displacement was around 10 pixels at each  $Ra_w$ .

A high pass filter was applied on the particle images, in order to make the varying background uniform. A stereo cross correlation method which calculates a 2D-3C vector field was used to evaluate the vector field. The size of the interrogation window was chosen so that there was a minimum of three velocity vectors within the plume thickness  $t_p$  at any  $Ra_w$  where,  $t_p$  was estimated from the similarity solutions for line plumes by Gebhart *et al.* (1970). Table 1 shows the values of  $t_p$  and  $L_v$ , the spatial resolution of velocity vectors at different  $Ra_w$ ; the number of vectors in  $t_p$  varied from about seven at the lowest  $Ra_w$  to about three at the highest  $Ra_w$ . The size of the interrogation window was also limited by the condition that the displacement due to the largest velocity in the horizontal plane was less than one fourth the interrogation window size and that a minimum of ten particles were present in the interrogation window for robustness of correlation. The bias errors were reduced by using a multipass adaptive window cross-correlation technique. Sub-pixel interpolation ensured that the peak lock value was less than 0.1, the acceptable limit of peak locking effect. The spurious vectors were removed by applying a median filter of  $3\text{pix} \times 3\text{pix}$  neighbourhood with interpolated vectors replacing the spurious vectors. A  $3\text{pix} \times 3\text{pix}$  smoothing filter was applied to the final vector field to reduce noise. Such smoothed images were used for the calculation of derivatives.

### 3. Extraction of line plumes from the velocity field

Figure 1b shows an example of the pattern of line plumes obtained by electrochemical dye visualization (Baker 1966) using Thymol blue at  $Ra_w = 7.5 \times 10^5$  (Gunasegarane & Puthenveettil 2014). Application of any criterion to detect coherent structures in turbulent convection should be first able to qualitatively reproduce the connected, line type of plume structure similar to that in figure 1b.

#### 3.1. Application of criteria from wall turbulence

We first apply the  $Q$ -criterion (Hunt, Wray & Moin 1988),  $\lambda_2$  criterion (Jeong & Hussain 1995) and the swirling strength ( $\lambda_{ci}$ ) criterion (Zhou, Adrian, Balachandar & Kendall 1999) on our velocity field to see whether the line plume structure is captured by these criteria. In all cases, the terms involving vertical velocity gradients are set to zero. The second invariant of  $\overline{\nabla \mathbf{u}}$ ,  $Q = \frac{1}{2}(\|\Omega\|^2 - \|S\|^2)$ , where  $\|\Omega\|$  and  $\|S\|$  are the symmetric and the anti-symmetric components of  $\overline{\nabla \mathbf{u}}$  respectively, is a local measure of excess rotation rate relative to the strain rate. Regions with  $Q > 0$  denote vortices and regions with  $Q < 0$  denotes regions of larger strain rate. Figure 2a shows the spatial map of  $Q$ , calculated from our 3D PIV vector field in a horizontal plane close to the plate, overlaid over the vector field at  $Ra_w = 7.66 \times 10^5$ . The regions of  $Q < 0$  captures line-like regions, into which the flow converges locally, which could be the plumes. However,  $Q < 0$  regions also include regions from which the flow diverges, namely regions at the center in between the

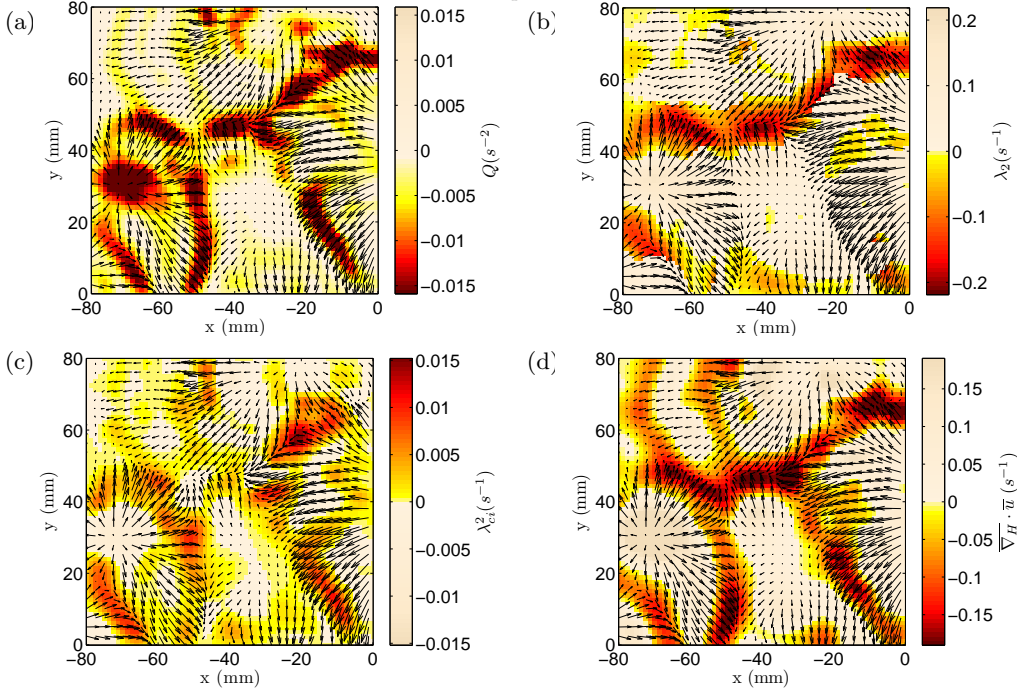


Figure 2: Coherent structure extraction methods applied on a vector field at  $Ra_w = 7.66 \times 10^5$ ; (a),  $Q$ -criterion; (b),  $\lambda_2$  criterion; (c),  $\lambda_{ci}$  method and (d),  $\overline{\nabla_H \cdot \bar{u}}$  criterion.

line-like regions, see at  $(-70, 30)$  and  $(-20, 70)$  in figure 2a, thereby making this criterion unsuitable for extracting plumes.

In  $\lambda_2$  criterion, the local pressure minimum within a vortex core is identified as the regions with two negative eigen values of the symmetric tensor  $\xi = \|\Omega\|^2 + \|S\|^2$ . Since the eigen values of  $\xi$  are real, from the ordered triad of the three local eigen values  $\lambda_1 \geq \lambda_2 \geq \lambda_3$ , the regions with negative  $\lambda_2$  are identified as the vortex cores. The  $\lambda_2$  criterion looks for the excess rotation rate relative to the strain rate in one plane alone while the  $Q$  criterion looks for it in all directions. Figure 2b shows the distribution of  $\lambda_2$  calculated from the vector field in figure 2a, overlaid over the same vector field. Far less line type structures are captured by the  $\lambda_2$  criterion, compared to that by the  $Q$  criterion, possibly because the terms set to zero in  $\xi$  are important in the present flow.

Swirling strength ( $\lambda_{ci}$ ) is the imaginary part of the complex eigen value of the velocity gradient tensor  $\overline{\nabla \bar{u}}$ , which is a measure of the local swirling rate inside a vortex. As shown in figure 2c, distribution of the positive values of  $\lambda_{ci}^2$  captures the line type structures. However, it also captures broad patches in various regions, like in locations  $(-60, 20)$ ,  $(-40, 5)$ ,  $(-25, 75)$  and  $(0, 40)$  in figure 2c, which do not seem to be plumes. It hence appears that  $Q$ ,  $\lambda_2$  and  $\lambda_{ci}$  criteria are not able to isolate plumes alone, mostly due to the non-availability of the vertical gradients of velocity, which seems to be important to correctly estimate the values of  $Q$ ,  $\lambda_2$  and  $\lambda_{ci}$  for the present flow. Since most PIV studies have the velocity field only in a horizontal plane and not in a 3D volume, as is often the case in numerical simulations where these criteria are more successful, these criteria can hence not be used to detect line plumes from PIV studies of turbulent convection. We now propose a new and simple criterion to detect line plumes from velocity fields in a plane parallel and close to the convecting surface.

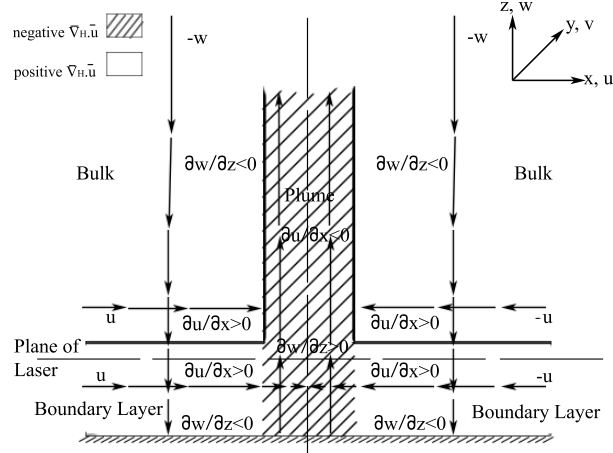


Figure 3: Schematic of the velocity variation in the plume, the bulk and the boundary layer.

### 3.2. $\overline{\nabla_H \cdot \bar{u}}$ criterion

#### 3.2.1. Physical justification

Plumes, shown as the hatched region in figure 3, are known to have positive vertical spatial acceleration,  $\partial w/\partial z > 0$  (Gebhart, Pera & Schorr 1970). At the same time, due to symmetry, horizontal velocities within the plumes decrease as we approach the center of the plumes from its edges, resulting in negative  $\partial u/\partial x$  in the hatched region of figure 3. Plumes do not occur in isolation, but cause flows around them due to the ambient fluid being entrained into them. Such entrainment flows are expected to have negative  $\partial w/\partial z$  since the large scale flow in the bulk is of an order higher in magnitude than the entrainment flows into the plumes and the boundary layers (Gunasegarane & Puthenveetil 2014). Hence,  $\partial w/\partial z$  is expected to be negative in the regions shown as bulk in figure 3. In addition, the presence of plumes also results in increasing horizontal velocities in the bulk ( $\partial u/\partial x > 0$ ) due to the entrainment, as shown by the horizontal arrows in the bulk region in figure 3. If we now consider regions within the boundary layers feeding the plumes on either sides at the bottom of the plumes, if these are natural convection boundary layers, the horizontal velocities are expected to increase towards the plumes since the driving horizontal pressure gradient increases with increase in boundary layer thickness ( $\Delta p \approx \rho g \beta \Delta T \delta_{nc}$ ) resulting in  $\partial u/\partial x > 0$ , as shown in the boundary layer regions in figure 3. Hence, we see that the flow near the plate separates into two regions, viz. (a) the plumes where  $\partial w/\partial z > 0$  and  $\partial u/\partial x < 0$  and (b) the bulk and the boundary layers where  $\partial w/\partial z < 0$  and  $\partial u/\partial x > 0$ ; these two regions are shown as the hatched and the unhatched regions respectively in figure 3. We hence need a criterion that distinguishes the  $\partial w/\partial z > 0$ ,  $\partial u/\partial x < 0$  regions as the plumes from the  $\partial w/\partial z < 0$ ,  $\partial u/\partial x > 0$  regions as the bulk or the boundary layer.

Horizontal, two dimensional divergence of the horizontal velocity components, calculated in a plane parallel and close to the plate,

$$\overline{\nabla_H \cdot \bar{u}} = \frac{\partial u}{\partial x} + \frac{\partial v}{\partial y}, \quad (3.1)$$

seems to satisfy the above mentioned requirements, with the subscript  $H$  indicating that the divergence operator is applied only on the horizontal ( $x$  and  $y$ ) components of the velocity field, namely  $u$  and  $v$ . Since the flow is incompressible,  $\overline{\nabla_H \cdot \bar{u}} = -\partial w/\partial z$ ;

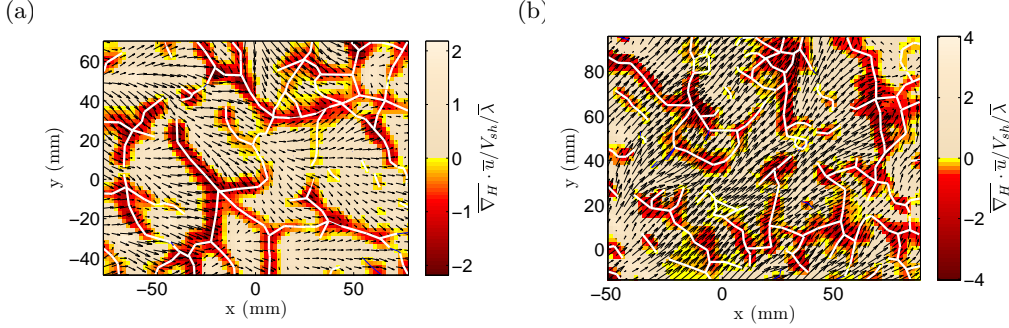


Figure 4:  $\overline{\nabla_H \cdot \bar{u}}$  overlaid over the 2D velocity field covered with short linear segments drawn over negative divergence regions at (a)  $Ra_w = 3.84 \times 10^6$ ,  $Pr=5.2$  and (b)  $Ra_w = 1.43 \times 10^9$ ,  $Pr=3.96$ .

negative values of  $\overline{\nabla_H \cdot \bar{u}}$  implies that such regions will have positive  $\partial w / \partial z$  and vice versa. Further,  $\overline{\nabla_H \cdot \bar{u}} < 0$  implies that these regions are also the regions in which the horizontal velocities reduce in magnitude along the direction of these velocities (figure 3). As we saw earlier, such regions are likely to be the plumes. Similarly, regions with  $\overline{\nabla_H \cdot \bar{u}} > 0$  will have increasing horizontal velocities in the direction of these velocities as well as  $\partial w / \partial z < 0$ ; such regions are more likely to be the ambient fluid or the boundary layer regions in between the plumes.

### 3.2.2. Verification of the $\overline{\nabla_H \cdot \bar{u}}$ criterion

We now apply this simple criterion to the horizontal velocity field obtained close to the plate in our experiments, on which the other criteria was applied in § 3.1. Figure 2d shows the instantaneous horizontal velocity field overlaid over the distribution of  $\overline{\nabla_H \cdot \bar{u}}$  calculated from the same velocity field using central differencing at  $Ra_w = 7.66 \times 10^5$ . Only the variations of negative  $\overline{\nabla_H \cdot \bar{u}}$  values are shown in dark color while all the positive values are set to a uniform grey color. Line like regions, similar to plumes, are detected by the  $\overline{\nabla_H \cdot \bar{u}}$  criterion. Unlike in the case of application of the  $Q$  criterion in figure 2a, the central, diverging flow regions between the plumes are not picked up by the  $\overline{\nabla_H \cdot \bar{u}}$  criterion. In comparison to the application of  $\lambda_2$  criterion in figure 2b, far more line like regions are picked up by the  $\overline{\nabla_H \cdot \bar{u}}$  criterion. A comparison of figures 2c and 2d shows that  $\lambda_{ci}$  picks up more line like regions than the  $\overline{\nabla_H \cdot \bar{u}}$  criterion, from which to identify the plumes the  $\lambda_{ci}$  criterion needs an unknown value of threshold for  $\lambda_{ci}$ . Hence, the negative values of  $\overline{\nabla_H \cdot \bar{u}}$  seems to fall on line like regions alone, which seems to be plumes, with no need for an arbitrary and a priori unknown threshold value for the criterion.

We now see whether the behaviour of such line like regions are qualitatively similar to that of line plumes. We define the dimensionless, two dimensional, horizontal divergence of the velocity field as,

$$\zeta = \frac{\overline{\nabla_H \cdot \bar{u}}}{V_{sh}/\bar{\lambda}} \quad (3.2)$$

where  $V_{sh}$  is the large scale velocity obtained from the shear Reynolds number,  $Re_{sh} = V_{sh}H/\nu = 0.55Ra_w^{4/9}Pr^{-2/3}$ , given as (5.2) in Gunasegarane & Puthenveetil (2014) and

$$\bar{\lambda} = C_1 Z_w Pr^{n_1} \quad (3.3)$$

is the mean plume spacing with  $C_1 = 47.5$ ,  $n_1 = 0.1$  and  $Z_w = (\nu\alpha/g\beta\Delta T_w)^{1/3}$  is

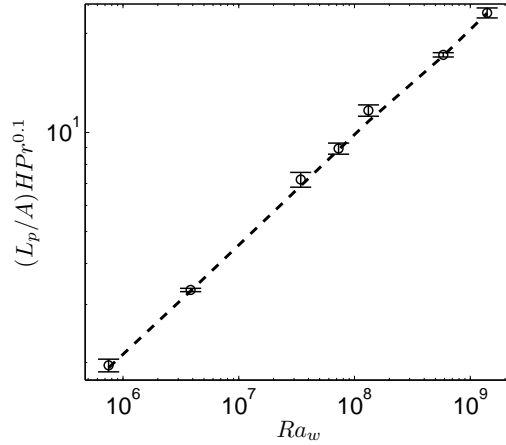


Figure 5: Comparison of the length of the negative  $\overline{\nabla_H \cdot \bar{u}}$  regions ( $\circ$ ) with the plume length given by (3.4) (---) for the range of  $Ra_w$  and  $Pr$  in the present experiments.

the length scale near the plate due to the balance of driving buoyancy forces and the dissipative effects; see Puthenveettil *et al.* (2011) for the physical significance of  $Z_w$ .

Figure 4 shows the distribution of the negative values of  $\zeta$  in dark color overlaid over the velocity vector field at  $Ra_w = 3.84 \times 10^6$  and  $Ra_w = 1.43 \times 10^9$ . Since the maximum value of  $\zeta$  is of order one,  $V_{sh}/\bar{\lambda}$  is the appropriate characteristic divergence of the velocity field. Figure 4b shows that an increase in  $Ra_w$  increases the length of the negative  $\zeta$  regions, as expected for line plumes (Puthenveettil *et al.* (2011)). At the lower  $Ra_w$  in figure 4a, the negative  $\zeta$  regions have flows going into them, as would be expected for plumes, since feeding of plumes by the boundary layers on their sides is predominant in the absence of strong large scale flows at lower  $Ra_w$  (Gunasegarane & Puthenveettil 2014). Figure 4 shows that, similar to line plumes, these regions also align along the predominant large scale flow direction in regions of stronger shear (Puthenveettil & Arakeri 2005). These qualitative considerations strongly suggest that the negative  $\zeta$  regions are the line plumes.

To quantitatively verify whether the  $\zeta < 0$  regions are plumes, we now compare the total length of the negative  $\zeta$  regions with the prediction of the total plume length in an area  $A$  of the hot plate,

$$L_p = A/\bar{\lambda}, \quad (3.4)$$

by Puthenveettil *et al.* (2011), where  $\bar{\lambda}$  is given by (3.3). Equation 3.4 has been verified with measurements of plume lengths over six decades of  $Ra_w$  and three decades of  $Pr$  by Puthenveettil *et al.* (2011). The length of the negative  $\zeta$  regions were measured as in Puthenveettil *et al.* (2011), by covering these regions with short linear segments as shown by the white lines in figure 4; the sum of the length of these segments gives the total length of the negative  $\zeta$  regions. Figure 5 shows the total length of the negative  $\zeta$  regions plotted along with (3.4) for the range of  $Ra_w$  in the present study. The error bars show the range of data from measurements at different instants at the same  $Ra_w$ . The excellent match between the theoretical prediction of  $L_p$  and the length of negative  $\zeta$  regions from the present measurements gives us confidence that these regions are the plume regions.

We now examine the thickness of the negative  $\zeta$  regions vis-a-vis the plume thickness. A qualitative examination of figure 2 shows that the thicknesses of the negative  $\overline{\nabla_H \cdot \bar{u}}$



regions are approximately the same as the plume thicknesses that would be identified by the other criteria. A quantitative comparison of the thickness of the plume region, identified by the  $\zeta < 0$  criterion, with the plume thickness in an ideal laminar line plume could be attempted as follows. The horizontal and vertical velocities in a laminar line plume are,

$$u = 4^{3/4} \frac{\nu}{z} Gr_z^{1/4} \left( \frac{3}{5} f'(\eta) - \frac{2}{5} \eta f(\eta) \right), \quad w = 4^{1/5} \left( \frac{g\beta Q}{C_p I} \right)^{2/5} \left( \frac{z}{\mu\rho} \right)^{1/5} f'(\eta), \quad (3.5)$$

where,  $Q$  is the heat flux per unit length of the line source,  $C_p$  is the specific heat at constant pressure,  $I = \int_{-\infty}^{\infty} f' \phi d\eta$  with  $\phi = (T - T_{\infty}) / (T_0 - T_{\infty})$  where  $T$  is the temperature with subscripts 0 and  $\infty$  denoting plume center line and ambient, and the similarity variable  $\eta = (x/z)(Gr_z/4)^{1/4}$  with  $Gr_z = g\beta(T_0 - T_{\infty})z^3/\nu^2$  being the Grashoff number based on  $z$  (Gebhart, Pera & Schorr 1970).  $f$  is the dimensionless stream function given by  $\psi = 4\nu(Gr_z/4)^{1/4} f(\eta)$ , with  $\psi$  being the stream function and  $'$  denotes differentiation with respect to  $\eta$ . The horizontal velocity in (3.5) shows that  $\partial u / \partial x$  is negative when  $\eta > f'(\eta) / 2f''(\eta)$  which is always satisfied within a plume since  $\eta$  is positive and  $f'(\eta)$  is a positive but a decreasing function with  $\eta$ . The vertical velocity in (3.5) reveals that, at any height  $z$ ,  $\partial w / \partial z = w / 5z = 0$  occurs at the same horizontal location as  $w = 0$ , corresponding to  $f'(\eta) = 0$ ; the ideal theoretical plume thickness calculated from  $w = 0$  and  $\zeta = 0$  would hence give the same value.

A comparison of the plume thicknesses obtained from the  $\zeta < 0$  criterion with that obtained from a threshold of dimensionless RMS temperature fluctuations  $\sigma = \sqrt{T'^2} / \Delta T$  has recently been attempted by Gastine *et al.* (2015). The plume regions identified by  $\overline{\nabla_H \cdot \bar{u}} < 0$  coincided with that identified by the  $\sigma$  criterion, however the plume thicknesses based on  $\sigma$  increased with decrease in  $\sigma$ , with  $\sigma = 0.25$  being close to, but slightly lower than, the thicknesses given by  $\zeta < 0$  criterion. They also showed that the PDF of the inter plume areas obtained by the  $\zeta < 0$  criterion has the same shape as that given by the threshold  $\sigma = 0.25$ , but is slightly shifted to the left. It hence appears that the thickness of the plume regions identified by the  $\zeta < 0$  criterion would be approximately equal to that estimated by a threshold of  $\sigma \approx 0.2$ .

#### 4. Conclusions

In this paper we showed that a simple criterion of  $\overline{\nabla_H \cdot \bar{u}} < 0$  picks up the plume regions in turbulent convection far better compared to the other criteria for detection of coherent structures from velocity fields alone, proposed for shear driven wall turbulence. The total length of plumes detected by such a criterion matched quite accurately with the available theoretical predictions of Puthenveetil *et al.* (2011). The thicknesses of the plume regions predicted by the criterion was approximately equal to that obtained by a threshold of  $\sqrt{T'^2} = 0.2\Delta T$  by Gastine *et al.* (2015); the plume regions coincided from both the criteria. The  $\overline{\nabla_H \cdot \bar{u}} < 0$  criterion was obtained from a physical picture of the flow induced by a line plume, where, due to the entrainment of the plume, regions outside the plume were expected to have increasing horizontal flow velocities as they approach the plume in a horizontal plane, resulting in positive values of  $\overline{\nabla_H \cdot \bar{u}}$ . However, in the presence of a strong external shear due to the large scale flow, which the line plumes in turbulent convection are subject to at high  $Ra_w$ , such positive spatial accelerations of the horizontal flows towards the plumes could be affected by the external shear, thereby affecting the thickness of the plume regions estimated by the  $\overline{\nabla_H \cdot \bar{u}} < 0$  criterion. In such situations, a modification of the present criterion to include the effect of the ambient

might be needed to get an accurate estimate of the plume thickness. However, such an effect would be negligible when the plane of analysis becomes close to the hot surface, as is in the present study, where the effects of large scale flow would be small even at high  $Ra_w$ .

## REFERENCES

- ADRIAN, R. J., FERREIRA, R. T. D. S. & BOBERG, T. 1986 Turbulent thermal convection in wide horizontal fluid layers. *Exp. Fluids* **4**, 121–141.
- AHLERS, G., GROSSMANN, S. & LOHSE, D. 2009 Heat transfer and large scale dynamics in turbulent rayleigh-bénard convection. *Rev. Mod. Phys.* **81**, 503–537.
- BAKER, J. D. 1966 A technique for the precise measurement of small flow velocities. *J. Fluid Mech.* **26** (3), 573–575.
- BELMONTE, A. & LIBCHABER, A. 1996 Thermal signature of plumes in turbulent convection: The skewness of the derivative. *Phys. Rev. E* **53**, 4893–4898.
- CHING, E. S. C., GUO, H., SHANG, X. D., TONG, P. & XIA, K. Q. 2004 Extraction of plumes in turbulent thermal convection. *Phys. Rev. Lett.* **93**, 124501.
- GASTINE, THOMAS, WICHT, JOHANNES & AURNOU, J. M. 2015 Turbulent Rayleigh-Bénard convection in spherical shells. *J. Fluid. Mech.* **778**, 721–764.
- GEBHART, B., PERA, L. & SCHORR, A. W. 1970 Steady laminar natural convection plumes above a horizontal line heat source. *Intl. J. Heat. Mass. Trans.* **13** (1), 161 – 171.
- GUNASEGARANE, G. S. & PUTHENVEETIL, B. A. 2014 Dynamics of line plumes on horizontal surfaces in turbulent convection. *J. Fluid. Mech* **749**, 37–78.
- HUNT, J. C. R., WRAY, A. A. & MOIN, P. 1988 Eddies, streams, and convergence zones in turbulent flows. In *Studying Turbulence Using Numerical Simulation Databases, 2*, pp. 193–208. Center for Turbulence Research, Ames Research Center.
- JEONG, J. & HUSSAIN, F. 1995 On the identification of a vortex. *Journal of Fluid Mechanics* **285**, 69–94.
- PUTHENVEETIL, B. A. 2004 Investigations on high Rayleigh number turbulent free-convection. PhD thesis, Indian Institute of Science, Bangalore, <http://etd.ncsi.iisc.ernet.in/>.
- PUTHENVEETIL, B. A., ANANTHAKRISHNA, G. & ARAKERI, J. H. 2005 The multifractal nature of plume structure in high-rayleigh-number convection. *J. Fluid. Mech* **526**, 245–256.
- PUTHENVEETIL, B. A. & ARAKERI, J. H. 2005 Plume structure in high-rayleigh-number convection. *J. Fluid. Mech* **542**, 217–249.
- PUTHENVEETIL, B. A., GUNASEGARANE, G. S., AGRAWAL, Y. K., SCHMELING, D., BOSBACH, J. & ARAKERI, J. H. 2011 Length of near-wall plumes in turbulent convection. *J. Fluid. Mech* **685**, 335–364.
- SHISKINA, O. & WAGNER, C. 2008 Analysis of sheet-like thermal plumes in turbulent rayleigh-bnard convection. *J. Fluid. Mech* **599**, 383–404.
- SPARROW, E. M. & HUSAR, R. B. 1969 Longitudinal vortices in natural convection flow on inclined plates. *J. Fluid. Mech* **37**, 251–255.
- TARDU, S. 2014 *Transport and Coherent Structures in Wall Turbulence*. Wiley.
- THEERTHAN, S. A. & ARAKERI, J. H. 1994 Planform structure of turbulent rayleigh-bnard convection. *Intl Commun Heat. Mass. Trans* **21** (4), 561 – 572.
- THEERTHAN, S. A. & ARAKERI, J. H. 1998 A model for near-wall dynamics in turbulent rayleighbnard convection. *J. Fluid. Mech* **373**, 221–254.
- ZHOU, J., ADRIAN, R. J., BALACHANDAR, S. & KENDALL, T. M. 1999 Mechanisms for generating coherent packets of hairpin vortices in channel flow. *Journal of Fluid Mechanics* **387**, 353–396.
- ZHOU, S. Q. & XIA, K. Q. 2002 Plume statistics in thermal turbulence: Mixing of an active scalar. *Phys. Rev. Lett.* **89**, 184502.